JOURNAL OF MATERIALS SCIENCE 29 (1994) 2921–2930

FTIR, DTA and XRD study of sphene ($CaTiSiO_5$) crystallization in a ceramic frit and a non-borate base glass

S. K. CHEN, H. S. LIU
Department of Mineral and Petroleum Engineering, National Cheng Kung University Tainan, Taiwan, Republic of China

The primary objective of this study has been the application of Fourier transform infrared (FTi.r.) absorption spectroscopy for both qualitative and quantitative characterization of sphene ($CaTiSiO_5$) crystallization in test materials; namely, a CaO–TiO_2–B_2O_3 bearing ceramic frit-S and a similar non-borate base glass-S. Differential thermal analysis (DTA), X-ray diffraction (XRD) and scanning electron microscope/electron probe X-ray microanalysis (SEM/EPMA) techniques have also been used. FTi.r. absorption spectra have been shown to be capable of providing both qualitative and quantitative characterizations of crystal nucleation and growth in a frit-S and glass-S, being annealed between 800–1100 °C. $CaTiSiO_5$ appears as the dominant phase and α-cristobalite as the transitional phase in frit-S; whereas, β-$CaSiO_3$ is dominant, $CaTiSiO_5$ being a minor phase in the non-borate glass-S. As given by DTA data, the intense stage of crystal growth for frit-S is about 120–125 °C lower than that of glass-S. B_2O_3 content and the relative amounts of CaO and TiO_2 in the test specimens have been shown to give different modes of phase evolution and the onset temperature of nucleation. The activation energies, E_c, of crystal nucleation/growth was estimated by two different methods, namely, via DTA data and FTi.r. absorption spectra under the dominant surface nucleation mode for powder pellet specimens. E_c for $CaTiSiO_5$, β-$CaSiO_3$ and α-cristobalite in the frit-S and the non-borate base glass-S were estimated to be 219.6, 107.2 and 51.5 kJ mol^{-1}, respectively, parallel to the decreasing order of chemical complexity of the glass-forming system. Similar quantitative FTi.r. studies in the determination of E_c for a broader scope of glass compositions, and compared with that based on XRD and DTA data, are to be encouraged so that the application of FTi.r. spectroscopy in glass–ceramics may be advanced.

1. Introduction

There has been growing interest in the application of FTi.r. and Raman spectroscopy in studying minerals and ceramic materials. The quantitative analysis of glass composition with the use of infrared reflection spectra for binary silicate glass has been demonstrated by Sanders *et al.* [1]. Whereas, the crystalline phases are generally characterized by X-ray diffraction (XRD) analysis, accurate quantitative analysis of crystal nucleation in the glassy precursors, and their transition towards crystalline materials by XRD, may be met with uncertainty due to intensive ionic rearrangements during the progressive course of annealing stages. Putnis and Bish [2] investigated the mechanism and kinetics of Al, Si ordering in Mg-cordierite ($Mg_2Al_4Si_5O_{18}$) glass during annealing by infrared (i.r.), transmission electron microscopy (TEM) and X-ray techniques. It is qualitatively illustrated that i.r. spectroscopy is necessary for elucidating the initial and transition stages of the growth of cordierite phase. On the other hand, the advanced FTi.r. spectrometer is considered to be capable of providing quantitative evaluations of crystalline phases [3, 4].

Ceramic frits are well known as a glassy silicate material consisting of a highly variable composition of inorganic oxides that fuse over a wide range of temperatures, namely, 500–1000 °C, resulting in the form of a flake product after supercooling the melt by water [5]. Frits have become indispensable in the industrial preparation of ceramic glazes for fulfilling protective and decorative purposes in ceramic products. By virtue of its uniqueness of complex chemical composition, ceramic frit may be used as a test material for the investigation of crystal nucleation and growth phenomena in glass–ceramics.

Sphene ($CaTiSiO_5$, also given as $CaTiOSiO_4$) is a complex orthosilicate mineral occurring in diverse geological environments [6]. Since it is possible to incorporate a variety of elements into the crystal lattice, sphene has been considered to be a candidate host material for the terminal fixation of radwaste via glass–ceramic processing into a synrock [7]. Hawthorne *et al.* [8] have studied alpha-decay damage in natural sphene from many sources by qualitatively correlating increasing structural damage (damage index) with decreasing crystallinity, by estimating the

0022–2461

decrease of peak heights in powder XRD patterns and powder i.r. spectra [from a single sharp (OH) stretching band at 3490 cm^{-1}]. Considering that this (OH) stretching band would become unavailable for characterization of $CaTiSiO_5$ crystallization in the annealed glass–ceramic bodies, there is a need to search for other appropriate i.r. bands. Hartman *et al.* [9] estimated the activation energy of crystallization of sphene via sol–gel and vitreous precursors to be about 300 kJ mol^{-1} by differential thermal analysis (DTA), for representing the total energy required for sphene, other intermediate and minor phases.

The primary objective of this study has been the application of FTi.r. absorption spectroscopy for both qualitative and quantitative characterization of sphene ($CaTiSiO_5$) nucleation and crystallization in the test materials in the form of powder pellet, namely, a $CaO–TiO_2–B_2O_3$ bearing ceramic frit and a similar non-borate base glass. XRD analysis provides phase identifications. In addition, differential thermal analysis (DTA) indicates the heat flow during the annealing treatment (800–1100 °C) of the test samples. The effects of B_2O_3 and (Al_2O_3 + TiO_2) content on the crystallization modes of sphene and other phases are noted. As a concluding consideration, an attempt is made to estimate the activation energies for crystallization of different phases, as sphene, β-wollastonite ($CaSiO_3$) and α-cristobalite (SiO_2), via data deduced from DTA and FTi.r. spectra.

2. Experimental

2.1. Test materials

Four test samples were used. Their sources, designation and preparation are given in the following.

2.1.1. Synthetic sphene

A batch bearing a stoichiometric composition was prepared from reagent grade $CaCO_3$, TiO_2 and SiO_2 compounds, by mixing, firing at 1300 °C for 4 h and cooling. Sphene was found, by XRD analysis, to be the only polycrystalline phase in the fired ceramic body. This sample serves as the standard for quantitative calibration of $CaTiSiO_5$ phase.

TABLE I Chemical composition of synthetic sphene, frit-S and glass-S

Chemical composition	Synthetic sphene [a] (wt %)	Frit-S [b] (wt %)	glass-S [c] (wt %)
CaO	28.6	10.0	14.4
Al_2O_3	–	4.0	5.7
TiO_2	40.8	5.8	8.3
SiO_2	30.7	44.9	64.4
Na_2O	–	4.5	6.5
K_2O	–	0.5	0.7
B_2O_3	–	29.8	–
P_2O_5	–	0.5	–

[a] Estimated.
[b] Batch formulated by mixing.
[c] Analysed by EPMA.

2.1.2. Natural wollastonite (β-$CaSiO_3$)

This is a white massively fibrous specimen, having high purity (> 99% $CaSiO_3$) and excellent crystallinity. Any notable impure grains were picked out by hand. This specimen is used as a wollastonite (β-$CaSiO_3$) standard for calibration.

2.1.3. Ceramic frit

Frit-S is a commercial frit, provided by a local ceramic glaze manufacturer. It is $TiO_2–CaO–SiO_2$ bearing, and is sphene ($CaTiSiO_5$) forming upon annealing. Its chemical composition is given by electron probe microanalysis (EPMA) shown in Table I.

2.1.4. Non-borate base glass

The material was prepared by mixing the reagent grade oxides of Na_2CO_3, $CaCO_3$, Al_2O_3, TiO_2 and SiO_2 according to the same ratio of the respective elements as in the composition of frit-S, but without B_2O_3 and P_2O_5 components. It was melted in an MgO crucible at 1400 °C for 4 h before pouring into de-ionized water, and a clear light amber coloured glass was obtained. The test sample is designated as glass-S.

2.2. Annealing treatment

The as-received frit-S and the glass-S test materials were ground to − 200 mesh with agate pestle and mortar. The powders were pressed into 10 mm discs under 250 MPa pressure. The discs were annealed separately at temperatures from 800, 850, 900, 950, 1000, 1050 and 1100 °C at a heating rate of 10 °C min^{-1} and at peak temperature dwell periods of 30 min. The annealed samples were furnace-cooled to room temperature.

2.3. Characterization

2.3.1. XRD

X-ray diffraction patterns were obtained using polished flat surfaces for all the annealed test samples by CuK_α radiation with nickel filter at a 2θ scanning rate of 1 ° min^{-1} on an X-ray diffractometer. Powder XRD patterns were also obtained for the synthetic sphene and natural wollastonite samples.

2.3.2. DTA

Thermal analysis of frit-S and glass-S were performed on the TAG24 of Setaram Co., France, from 70 to 1200 °C at a ramp rate of 20, 25, 30 and 35 °C min^{-1} in open air in a platinum crucible. The sample weight was 40 mg, and Al_2O_3 powder was used as the reference material.

2.3.3. SEM/EPMA

The chemical composition of frit-S was analysed by energy dispersive spectroscopy (EDX) on a scanning electron microscope (SEM type S-405A). Scanning

electron micrographs of the etched polished surface of annealed frit-S and glass-S were taken on a SEM.

2.3.4. FTi.r. absorption spectra

I.r. absorption spectra were obtained by processing on an optical bench of the standard Nicolet's System 800 Fourier transform infrared spectrometer, featured with an SX operation system, on a Model 620 workstation. A spectral resolution of 4 cm^{-1} was chosen. Each test sample was mixed with KBr (1 wt % of former), and was pressed into 200 mg pellets, of 13 mm diameter, for taking infrared absorption spectra at a frequency range of 400–4000 cm^{-1}. The composite spectrum for each sample represented an average of 64 scans, normalized to the spectrum of the blank KBr pellet.

Quantitative evaluation of the $CaTiSiO_5$ and β-$CaSiO_3$ phase in each test sample was performed on the absorption spectra using calibration plots by the classical least square method (CLS), obtained by using high purity/crystallinity material standards, such as synthetic sphene and natural wollastonite. The peak height of sphene absorption bands at 561 cm^{-1} SiO_4, and of β-$CaSiO_3$ at 566 cm^{-1} SiO_4 have been adopted for calibration. The amount of crystalline phases in the annealed specimens was derived from the calibration plots.

3. Results

Evolution of a crystalline phase and crystal growth of frit-S and glass-S have been investigated by employing DTA, XRD, SEM and FTi.r. techniques. Results are described separately as follows.

3.1. Thermal analysis

A representative DTA result for frit-S, at a heating rate of 20 °C min^{-1} is given in Fig. 1a. It shows a low broad endothermic peak indicating glass transition starting at 640 °C and ending at 820 °C, and a second, but smaller, endothermic region between 950–1040 °C. A very broad exothermic region has been observed between 820–1100 °C, including a reduced exothermic region between 1040–1100 °C. This may be separated into two sub-regions, dividing at around 1010 °C. DTA results for glass-S, at a heating rate of 20 °C min^{-1}, are shown in Fig. 1b. The glass transition starts at around 680 °C, and a very broad exothermic region is noted between 870–1150 °C. The peak at 970 °C is prominent. Apparently, frit-S and glass-S have different crystallization modes. On the other hand, thermographs were also obtained for three other different heating rates of 25, 30 and 35 °C min^{-1}; the exothermic peak temperatures for the different heating rates for frit-S and glass-S are given in Table II. Generally speaking, the exothermic peak temperature for frit-S is about 120–125 °C lower than that for glass-S. No significant weight losses could be observed in the range of test temperatures for both samples.

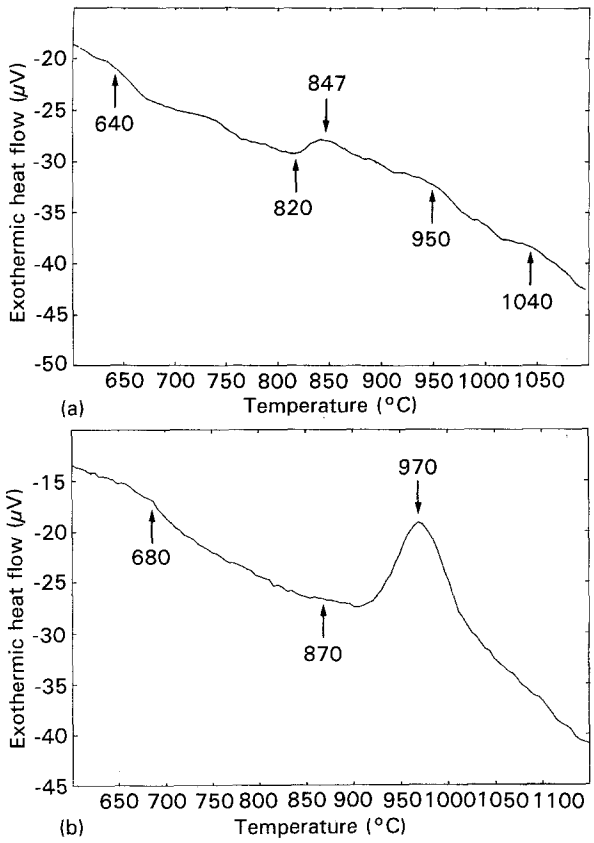

Figure 1 Representative DTA curves taken at a heating rate of 20 °C min^{-1} for (a) frit-S and (b) glass-S.

TABLE II Exothermic peak temperatures of frit-S and glass-S at different heating rates

Heating rate (°C min^{-1})	Frit-S (°C)	Glass-S (°C)
20	846.9	971.5
25	856.9	979.1
30	864.7	983.6
35	867.9	993.9

3.2. XRD analysis

Based on the XRD results, two crystalline phases appear in the annealed frit-S samples. Sphene is the first crystalline phase nucleated in frit-S, with an onset crystallization temperature at 800 °C. α-cristobalite (SiO_2) as a secondary and intermediate phase emerges at 850 °C, maturing between 900–950 °C. Surprisingly, α-cristobalite disappears in the XRD patterns for annealing temperatures of 1000 °C or above. The X-ray diffractograms of frit-S annealed from 800 to 1050 °C are plotted in Fig. 2. It is easily noted that the XRD peak intensities of sphene have not increased significantly with increasing annealing temperature. Accordingly, these XRD patterns could not be employed easily as a basis for the quantitative determination of crystalline phases.

XRD results for glass-S annealed between 850–1100 °C are given in Fig. 3. There are also two crystalline phases noted from the XRD patterns of the annealed glass-S samples. Simultaneous crystallization of $CaTiSiO_5$, as a minor phase, and β-$CaSiO_3$, as

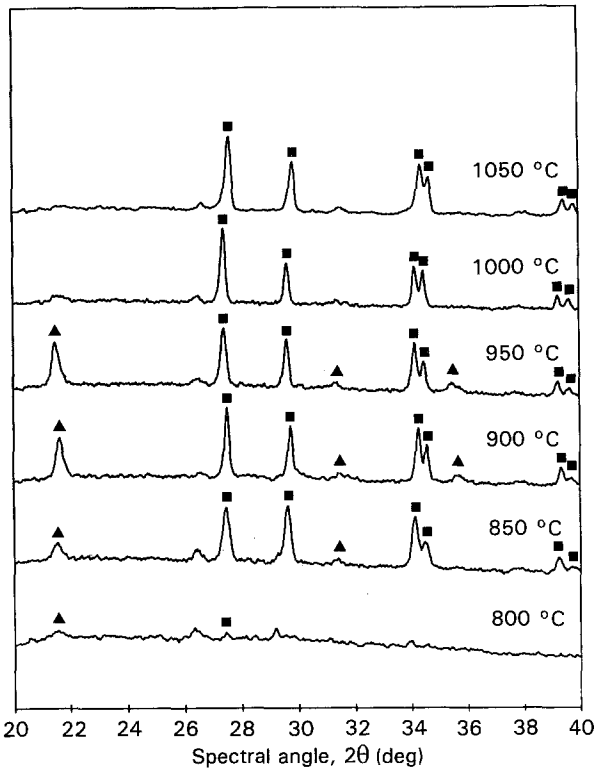

Figure 2 XRD patterns of frit-S annealed from 800 to 1050 °C for 30 min dwell time at peak temperatures: (■) sphene, (▲) α-cristobalite.

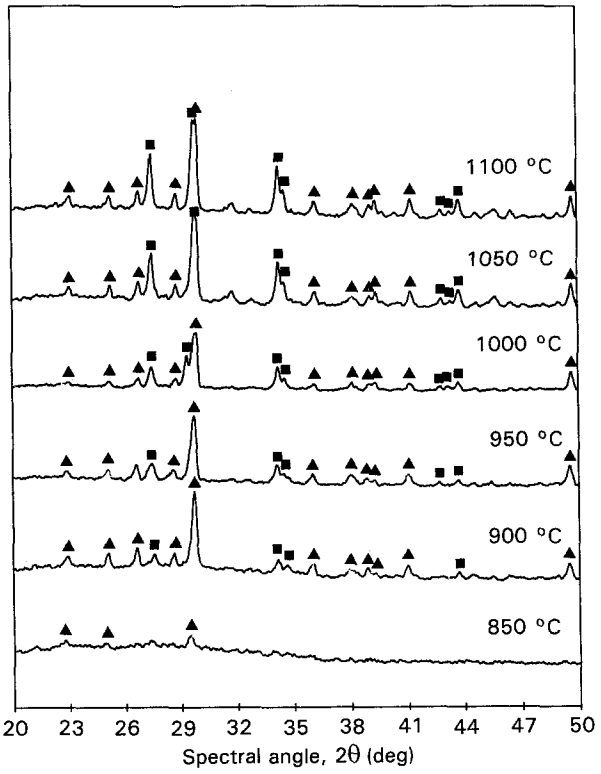

Figure 3 XRD patterns of glass-S annealed from 850 to 1100 °C for 30 min dwell time at peak temperatures: (■) sphene, (▲) wollastonite.

the major phase, is shown; no α-cristobalite is noted as in the case of frit-S. The β-$CaSiO_3$ phase appears to nucleate at around 850 °C, and grows steadily from 900 to 1100 °C. However, the peak heights of the β-$CaSiO_3$ XRD patterns are more or less similar at most 2θ positions for each annealing temperature, thus failing to serve as a parameter for quantitative determination. On the other hand, the minor $CaTiSiO_5$ phase appears to nucleate at around 900 °C, and the peak heights for $CaTiSiO_5$ increase steadily with increasing temperature until 1100 °C. Therefore, the crystallization modes for phase evolution are quite different between frit-S and the closely related non-borate base glass-S. Furthermore, more elaborate experimentation, using a comprehensive programme for heat treatment with respect to heating rates and longer soaking times, are needed for finding an explanation for similar peak heights of the major phases under different annealing temperatures.

3.3. SEM observations

The SEM micrographs, as shown in Fig. 4a–d, are a selection of results showing nucleation and maturing crystal growth for frit-S and glass-S. In the case of frit-S at 850 °C, $CaTiSiO_5$ is noticeably nucleated along grain boundaries (greyish areas); crystal sizes are variable, mostly less than 1 μm. Within the grain bodies (whitish areas), globular cavities of various sizes, < 2.0 μm, are evenly distributed. It is remarkable that $CaTiSiO_5$ crystal sizes are greater, and are located in proximity to grains having larger cavities. This phenomenon seems to indicate that diffusion of nutrients from the feedstock grain promotes $CaTiSiO_5$ nucleation and growth along grain boundaries with the concomitant development of cavities, showing loss of material. At 1050 °C, $CaTiSiO_5$ crystals, 1–3 μm, are mostly peanut shaped, being aligned *en echelon* into feather-like morphologies; the residual glass phase covers more than 50% of the exposed area.

For the non-borate base glass-S at 850 °C, nuclei along intergranular boundaries are obvious; $CaSiO_3$ nuclei appear in two forms, as globular aggregates, about 5 μm in size, and as 2–3 μm-sized nuclei. $CaTiSiO_5$ nucleation seems to be hardly noticeable as small whitish nuclei, about 0.5–1.0 μm in size. At 1050 °C, long acicular β-$CaSiO_3$ crystals, 15–30 μm in length, are predominant; cavities in bright spots represent the position/shape of detached sphene crystals after etching; residual glass matrix appears to occupy less than 40% of the exposed area.

Fig. 4b, d shows that nucleation occurs along grain boundaries, and crystal growth is extended intragranularly. The crystal sizes along boundaries are much more crowded and smaller than those within the grains. Thus, heterogeneous nucleation along intergranular boundaries appears to be the dominant mode of crystallization. For both frit-S and the non-borate base glass-S, the maturing sizes of $CaTiSiO_5$ crystals, mostly between 1–3 μm in length and 0.5–1.0 μm in width, are much smaller than that of β-$CaSiO_3$.

3.4. FTi.r. absorption spectra

FTi.r. absorption spectra for the mid i.r. range of 400–1800 cm^{-1} of the frit-S and the non-borate base glass-S, annealed between 800–1050 °C, and that of the high purity/crystallinity material standards of

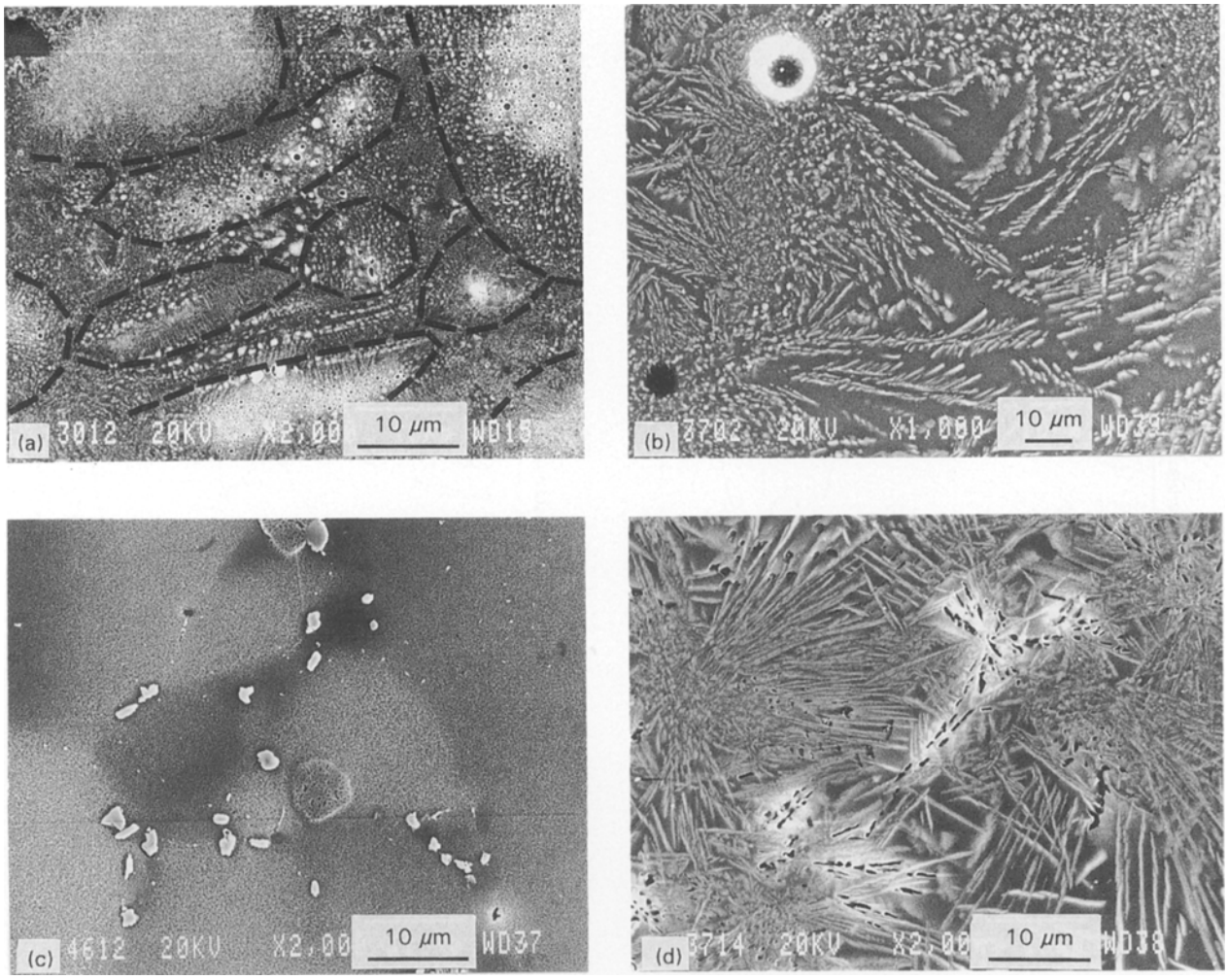

Figure 4 Micrographs of the etched and polished surface of annealed frit-S at (a) 850 °C, (b) 1050 °C; and glass-S at (c) 850 °C, and (d) 1050 °C. In (d), the cavities in bright areas represent positions of etched-out $CaTiSiO_5$ crystals.

$CaTiSiO_5$ and β-$CaSiO_3$ used for constructing calibration graphs are given in Figs 5 and 6, respectively. It may be generalized that the effect of annealing temperature on the i.r. spectra is obvious, in that the broad i.r. bands become more resolved and render increasing peak heights with increasing temperature. As expected, the standard materials having high purity/crystallinity give much sharper i.r. absorption spectra. This general trend may be thus considered to be most helpful in the quantitative characterization of chemical groupings, as directly related to nucleating and growing phases undergoing chemical and lattice rearrangement.

The precise band assignments of the i.r. absorption spectra for our test samples, as frit-S and glass-S in having very complex chemical compositions, are obviously quite difficult [9]. This task is made simpler by using high purity/crystallinity specimens as standards for calibration. Thus, by detailed searching of previously published i.r. spectral data, the following approximate band assignments in the empirical spectra are briefly given.

As expected, simple chemistry, as in case of the material standards used, gives definitely resolved bands; whereas, the complex chemical composition of frit-S and glass-S render very broad and faintly resolved peaks. I.r. absorption spectra between 400–1800 cm^{-1} may be divided into four major band areas: (i) 400–600 cm^{-1}; (ii) 600–800 cm^{-1}; (iii) 800–1200 cm^{-1}; and (iv) 1200–1800 cm^{-1}, given in the following.

(i) 400–600 cm^{-1}: The region between 400–500 cm^{-1} may be attributed to the bending vibrational modes of Si–O–M, in which M = Si or Al. In particular, the bands between 560–570 cm^{-1} in the standard materials, as well as in annealed frit-S and glass-S, are sharper but of low peak height. This has a special significance, and may be assigned to the "internal vibration mode" of SiO_4 tetrahedra of the crystallized silicate phases in $CaTiSiO_5$ and β-$CaSiO_3$ [10–13].

(ii) 600–800 cm^{-1}: A direct comparison between the spectra for $CaTiSiO_5$ and β-$CaSiO_3$ shows that a broad band in this interval, with a peak located at 676 cm^{-1}, is due to vibrational modes of TiO_6 in sphene; whereas, for β-$CaSiO_3$, two separate sharp peaks appear at 644 and 681 cm^{-1}, attributed to SiO_4 vibrations. AlO_4 vibration modes are also located, presumably peaking at $\sim$ 720 cm^{-1} [13]. With reference to the claim of Gabelica-Robert and Tarte, by employing isotopic discrimination [14] the peak at around 675–680 cm^{-1} may represent the vibration of Ti–O short bonds in TiO_6 groups; this particular peak appears as a shoulder to the broad band in this interval.

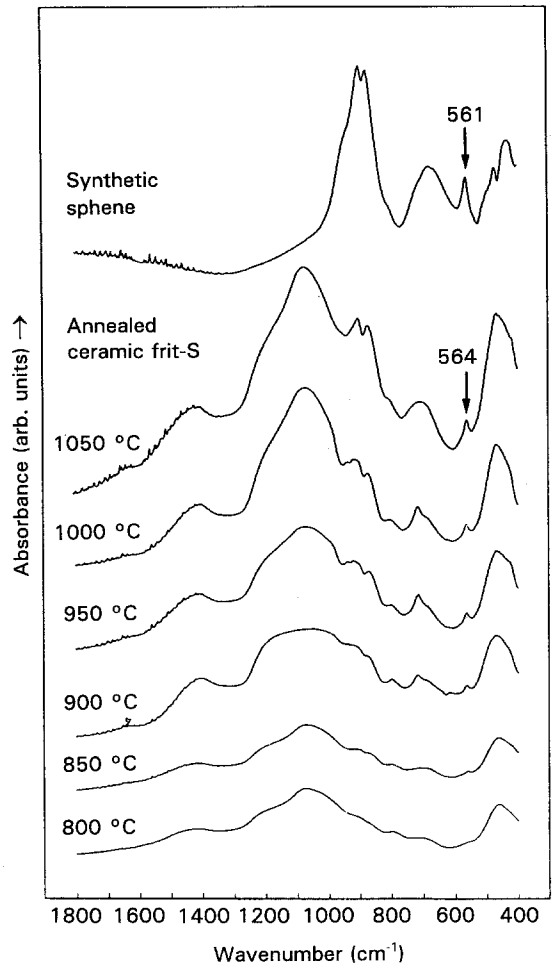

Figure 5 FTi.r. absorption spectra (400–1800 cm^{-1}) of ceramic frit-S annealed at 800–1050 °C and synthetic sphene ($CaTiSiO_5$) standard.

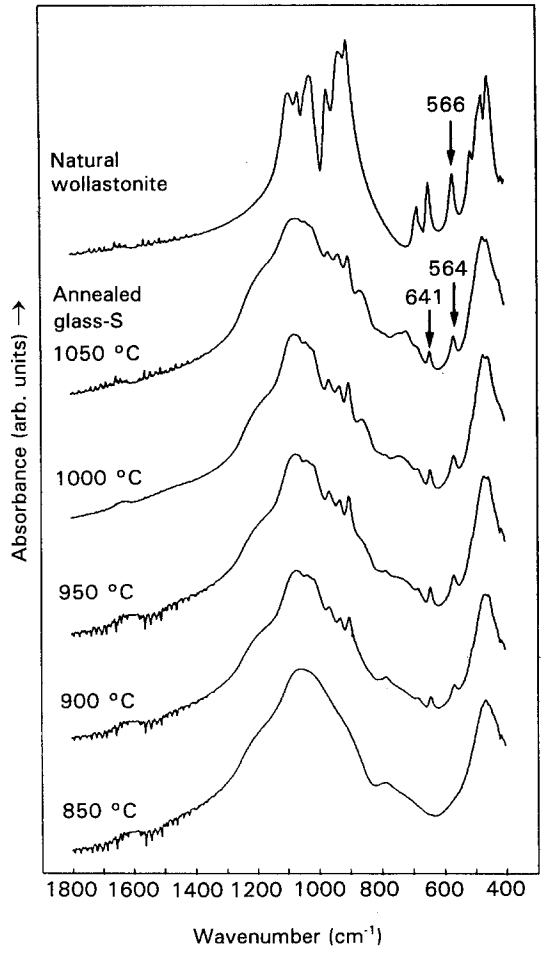

Figure 6 FTi.r. absorption spectra (400–1800 cm^{-1}) of ceramic glass-S annealed at 850–1050 °C and natural wollastonite (β-$CaSiO_3$) standard.

(iii) 800–1200 cm^{-1}: For all test specimens, the band between 800–1200 cm^{-1} gives prominently broader and taller peaks. This is indicative of the complexities of the stretching modes of lattice vibrations involving Si–O–M, in which M = Si, Al and Ti [15–19].

(iv) 1200–1800 cm^{-1}: Frit-S shows a low broad band at about 1400 cm^{-1}, which is not present in the non-borate base glass-S, synthetic $CaTiSiO_5$ and natural β-$CaSiO_3$. This is attributable to the vibration mode of BO_4 [17].

TABLE III Intensity of nucleation of crystal growth in annealed frit-S and glass-S at various temperatures. Relative degree of crystal growth: (↑) initial/low, (↑↑) moderate, (↑↑↑) intense, and (↓) dissolving in glass matrix

Temperature (°C)	800	850	900–950	1000	1050	1100
Frit-S						
Sphene	↑	↑↑	↑↑	↑↑↑	↑	↑
α-cristobalite	↑	↑↑	↑↑↑	↓	–	–
Glass-S						
β-$CaSiO_3$	–	↑	↑↑	↑↑	↑↑↑	↓
Sphene	–	↑	↑	↑	↑	↑

4. Discussion

This study has explored two particular areas of pursuit: (a) quantitative characterization of $CaTiSiO_5$ and β-$CaSiO_3$ nucleation and growth by FTi.r. absorption spectra, and (b) the estimation of crystallization activation energies of $CaTiSiO_5$, β-$CaSiO_3$ and α-cristobalite via DTA and FTi.r. data. Limited by the scope of experimentation, as to conditions of testing and choice of crystal chemistry, the findings given here must be considered to be a preliminary conclusion and further studies based on a similar approach are to be encouraged. The results are discussed in order of: (i) nucleation and crystal growth; (ii) quantitative analysis by FTi.r. absorption spectra, and (iii) activation energies of crystallization.

4.1. Nucleation and crystal growth

Table III is an overview of the nucleation and relative growth intensity of different crystalline phases in frit-S and similar non-borate base glass-S from XRD and FTi.r. results, being annealed between 800–1100 °C. The dominant $CaTiSiO_5$ phase is being promoted in the case of frit-S, as opposed to $CaTiSiO_5$ being developed as a minor phase in a related non-borate base glass-S. As an aid for melting point depression for glass–ceramics, the effect of B_2O_3 in phase evolution is evident, in that in the B_2O_3-bearing frit-S, $CaTiSiO_5$ nucleates at 800 °C, whereas, in the non-borate base glass-S, β-$CaSiO_3$ and $CaTiSiO_5$ nucleate at about 850 and 900 °C from XRD data, respectively. As given in Table II, the exothermic peak

temperatures for frit-S are generally 120–125 °C lower than those of glass-S, suggesting that the intense stage of crystal growth in frit-S occurs at much lower temperatures than in glass-S. This compositional effect of the relative predominance of phase evolution between β-$CaSiO_3$ and $CaTiSiO_5$, based on the relative amounts of $CaO:TiO_2$, may also be noted from the $CaO–TiO_2–SiO_2$ phase diagram of DeVries *et al.* [20]; they indicate that a higher $CaO:TiO_2$ content tends to favour β-$CaSiO_3$ as in glass-S, whereas in frit-S, a lower $CaO:TiO_2$ ratio supports $CaTiSiO_5$ crystallization. In the development of sphene glass–ceramics for nuclear waste fixation, Hayward *et al.* [21] showed a $Na_2O–CaO–Al_2O_3–TiO_2–SiO_2$ base glass, having 18.30 wt % TiO_2 and 14.32 wt % CaO, in which a sole $CaTiSiO_5$ phase was crystallized.

As in the case of frit-S, α-cristobalite, generally noted as a high temperature crystalline form of SiO_2, emerges and finally phases out at about 850 °C and 1000 °C, respectively. This disposition may be explained in the same way as Buerger's work [22] on the crystallization of SiO_2 melt, i.e. Na_2O, CaO and other impurities are favourable for the development of α-cristobalite at much lower temperatures than expected. Zarzycki [23] also showed that α-cristobalite crystallized in a 95 wt % SiO_2–5 wt % B_2O_3 glass from a gel precursor at 850 °C, and SiO_2 gel with about 3 wt % Na_2O also facilitates α-cristobalite crystallization at 900 °C. α-cristobalite is shown to occur as a trace crystalline phase for a heat-treated sol–gel $CaTiSiO_5$ precursor between 800 and 1000 °C.

The SEM micrographs, shown in Fig. 4, for both frit-S and glass-S, in the form of powder pellets prior to annealing, seem to indicate that heterogeneous nucleation along intergranular boundaries, or simple surface nucleation, is the dominant mode of nucleation, and that crystal growth extends into the interior of grain bodies. Phase separation into $Na_2O–Al_2O_3–SiO_2$ and $CaO–TiO_2–SiO_2$ enriched phases prior to nucleation cannot be discerned from the micrographs. The results are similar to that of Hayward *et al.* [21], i.e. sphene nucleated along granular boundaries in a $Na_2O–CaO–Al_2O_3–TiO_2$ base glass, but with the prior step of phase separation.

4.2. Quantitative analysis by FTi.r. absorption spectra

The absorption spectra, as given in Figs 5 and 6, have so clearly shown the direct relationship between annealing temperature and crystal nucleation and growth as to inspire the authors' attention in applying these spectra for quantitative evaluation purposes. Therefore, using the high purity/crystallinity $CaTiSiO_5$ and β-$CaSiO_3$ specimens, calibrations are attempted for relating peak height for certain specific FTi.r. absorption bands versus the amount (wt %) of crystallized phase. The peak at 561 cm^{-1} for SiO_4 has been selected for sphene ($CaTiSiO_5$) and 566 cm^{-1} for SiO_4 for wollastonite (β-$CaSiO_3$). Using the classical least square method, calibration graphs give correlation coefficients of 0.9964 and 0.9937 for SiO_4 from sphene and wollastonite, respectively. Details of calibration results are given in a separate paper [4].

Amounts of crystallized phases in test specimens are then estimated for each annealing temperature. The relationship between the amount (wt %) of crystallized phase versus annealing temperature is given in Table IV. The temperatures of peak crystal growth are 1000 and 1050 °C for $CaTiSiO_5$ in frit-S and β-$CaSiO_3$, in non-borate base glass-S, respectively. α-cristobalite does not possess an absorption band between 560–570 cm^{-1}. At this stage of the study positive identification of possible error in the results for quantitative evaluation is yet to be determined, since the absorption bands for $CaTiSiO_5$ and β-$CaSiO_3$ for glass-S almost coincide with each other in the 560–570 cm^{-1} range, the spectra resolution being chosen at 4 cm^{-1}. However, using the unique 641 cm^{-1} peak for β-$CaSiO_3$, the amount of $CaTiSiO_5$ for specimens annealed at 1050 °C has been indirectly estimated to be 3–4 wt %.

4.3. Activation energies of crystallization

Activation energy for crystal nucleation and growth may be estimated by two different methods, separately based on the concept of the volume fraction of the crystallized phase from FTi.r. results and heat quantities involved from DTA results. For this study, both methods are being employed, as FTi.r. absorption spectra giving wt % crystallized phases, and DTA curves giving heat flow yields. The estimated values of crystallization activation energies may be thus compared.

4.3.1. Based on DTA data

Crystalline phase evolution from a glassy state is generally considered to be an exothermic process that will show up on the DTA curve. The mode of nucleation, namely surface (grain boundary) versus bulk, is a prerequisite for evaluation of activation energy of crystal nucleation/growth. In the case of surface nucleation, the morphology index being 1.0, the temperature of exothermic peaks at various heating rates may be related to the activation energy of crystallization by the Arrhenius equation modified by Marotta

TABLE IV Quantitative analysis of crystallized $CaTiSiO_5$ and β-$CaSiO_3$ in frit-S and glass-S at different annealing temperatures by i.r. absorption peak heights at 564 cm^{-1} [3]

Annealing temperature (°C)	Frit-S[a], $CaTiSiO_5$, (wt %)	Glass-S[a], β-$CaSiO_3$ (wt %)
800	1.15	–
850	4.46	–
900	11.25	13.68
950	21.13	20.36
1000	24.86	26.95
1050	16.25	41.14
1100	18.16	26.40

[a] Correlation coefficients of calibration plots have been given as 0.9964 and 0.9937 for frit-S and glass-S, respectively, in Reference 4.

et al. [24, 25]

$$\ln h = -\frac{nE_c}{R}\frac{1}{T_p} + K = -\frac{E_c}{R}\frac{1}{T_p} + K \quad (1)$$

where h is the heating rate, E_c the activation energy of crystallization, T_p: the peak temperature, and K a constant. The activation energy of crystallization may be then deduced from the slope of the plot ln h versus $1/T_p$, as shown in Fig. 7a, b for frit-S and glass-S, respectively, based on data given in Table II. When more than one crystalline phase is involved, E_c represents all these phases. Then, E_c for $CaTiSiO_5$ + α-cristobalite in frit-S and $CaSiO_3$ + $CaTiSiO_5$ in the non-borate base glass-S is 271.1 ± 27 and 331.2 ± 47 kJ mol^{-1}, respectively. Hayward *et al.* [21] indicate that the E_c estimates by the DTA method could be uncertain due to various reasons, particularly, the variable factor of surface versus bulk crystallization.

4.3.2. Based on FTi.r. data

According to the Johnson–Mehl–Avrami (JMA) method [24, 25], crystal growth may be expressed by the following equation

$$-\ln(1\text{-}C) = (kt)^n \quad (2)$$

where C is the volume fraction of crystallized phase at time t, and n is a morphology index ($n = 1$, surface crystallization; $n = 3$, bulk crystallization). The k constant is related to absolute temperature, T, by an Arrhenius equation,

$$k = AN\exp(-E_c/RT) \quad (3)$$

where E_c is the activation energy for crystal growth, N the number of nuclei, and A is a constant. By combining Equations 1 and 2, Equation 4 is obtained as:

$$\ln\left[\frac{1}{\ln(1-C)}\right] = n[\ln(ANt) - E_c/RT] \quad (4)$$

Using powder pellets during experimentation, annealing time has been fixed at 30 min and the crystallization mode appears, from SEM observations, to be heterogeneous surface nucleation. As in this case, the morphology index, n, is taken to be 1.0; Equation 4 is then reduced to

$$\ln\left[\frac{1}{\ln(1-C)}\right] = K - E_c/RT \quad (5)$$

The activation energy of nucleation and crystal growth could be derived from slope ln [1/ln(1 − C)] versus $1/T$. Using data from quantitative analysis shown in Table IV, plots of ln [1/ln(1–C)] versus $1/T$ for crystallization of $CaTiSiO_5$ and β-$CaSiO_3$ are given in Fig. 8. The crystallization activation energies based on DTA and FTi.r. data are given in Table V. E_c

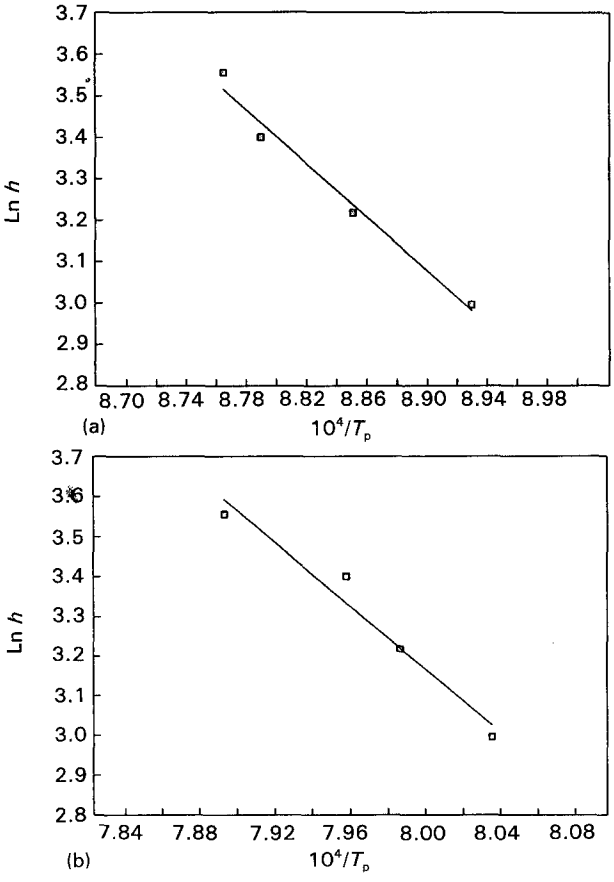

Figure 7 Plot of ln h versus $1/T_p$ based on DTA data for (a) frit-S, correlation coefficient = 0.981, and (b) glass-S, correlation coefficient = 0.961.

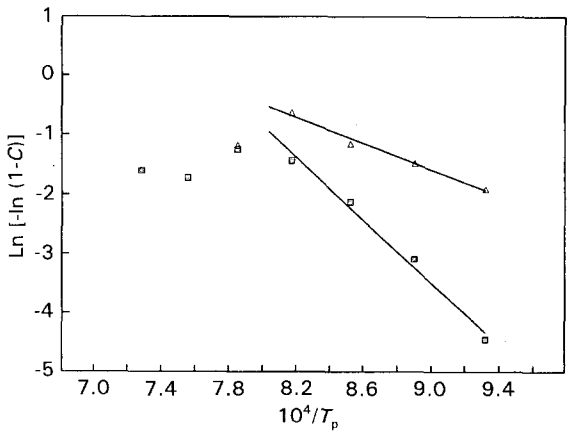

Figure 8 Plots of ln [1/ln(1 − C)] versus $1/T$ based on crystallized amounts of sphene and β-wollastonite in (■) frit-S and (▲) glass-S by FTi.r. absorption spectra; correlation coefficient = 0.987 for glass-S and 0.987 frit-S.

TABLE V Activation energies, E_c, of nucleation and crystal growth of sphene, wollastonite and α-cristobalite phases in frit-S and glass-S based on DTA and FTi.r. data

Crystalline phases	Activation energy (kJ mol^{-1})		
	FTi.r.	DTA	Derived
Frit-S			
Sphene[a]	219.6 ± 18	–	–
Sphene + α-cristobalite	–	271.1 ± 27	–
α-Cristobalite[b]	–	–	51.5
Glass-S			
Wollastonite[a]	107.2 ± 8	–	–
Wollastonite + sphene	–	331.2 ± 47	–
Sphene[b]	–	–	224.0

[a] Major phase.
[b] Minor phase.

for $CaTiSiO_5$ in frit-S and β-$CaSiO_3$ in glass-S are given as 219.6 ± 18 and 107.2 ± 8 kJ mol^{-1}, respectively.

4.3.3. E_c deduced for minor phases

One advantage of the method, via FTi.r. data, is that E_c for a single specific phase may be estimated by a unique absorption peak. By comparing the results between two different methods, the activation energies of minor phases, such as α-cristobalite in frit-S and $CaTiSiO_5$ in glass-S, could be estimated indirectly, as 51.5 and 224.0 kJ mol^{-1}, respectively. This indirect method for deducing E_c for mixed phase evaluation in annealed glass appears to be useful in characterization of thermal quantities of crystal nucleation and growth in glass–ceramics.

4.3.4. Comparison of E_c values from DTA/FTi.r.

A useful outcome of the above discussion is a beneficial comparison of E_c crystallized phase values from DTA and FTi.r. absorption spectra data. Thus, E_c for sphene ($CaTiSiO_5$) from test materials with a more or less similar chemistry are separately derived as: (a) 219.6 ± 18 kJ mol^{-1} in frit-S, directly based on FTi.r. data, and (b) 224.0 kJ mol^{-1} in the non-borate base frit-S, indirectly derived. The difference between the two values is noted to be quite low, being a mere 2%. Using DTA data, bulk nucleation mode ($n = 3$) and a Kissinger-type equation, Hayward *et al.* [21] showed E_c for sphene crystallization in a base–glass versus simulated high level waste (SHLW) glass are 461 and 471 kJ mol^{-1}, respectively, or a difference of about 2.5% between the two values. As shown by Hartman *et al.* [9], E_c for sphene, intermediate and minor phases from sol–gel and vitreous $CaTiSiO_5$ precursors, are given as 315 and 335 ± 30 kJ mol^{-1}, respectively.

It may be seen that the activation energies for crystal nucleation/growth in this study and in Hayward *et al.* [21] have an approximate ratio of 1:2. A full explanation for the difference in E_c values between the two studies cannot be provided here. However, it may be pointed out that the glass-S sample used in this study has much lower (Al_2O_3 + TiO_2) content, 14%, than that of Hayward's, 26.4%; therefore, the former is expected to have much lower viscosities than the latter, thus giving a lower E_c value. In a critical review of nucleation in glass-forming systems, James [26] considers that surface nucleation occurs more easily than volume or bulk crystal nucleation. Furthermore, Wang and Hon [27] have shown that E_c for $CaTiSiO_5$ catalysed spodumene ($LiAlSi_2O_6$) glass–ceramics varied from 151.9 to 249.4 kJ mol^{-1}. Apparently, further comprehensive studies are needed to find a sound explanation for the substantial differences in E_c values noted between different studies.

5. Conclusions

1. In multicomponent glass forming systems, such as frit-S and a similar non-borate base glass-S, annealed between 800–1100 °C, the dominant crystalline phases identified by XRD analysis are sphene ($CaTiSiO_5$) and wollastonite (β-$CaSiO_3$), respectively; sphene is the minor phase in glass-S, and α-cristobalite appears as the transitional phase (between 850–950 °C) in frit-S. As given by DTA data, the intense stage of crystal growth in frit-S occurs at about 120–125 °C lower than that for glass-S. B_2O_3 content and the relative amount of CaO and TiO_2 in the test materials are considered to have caused the different modes of phase evolution and the onset temperature of nucleation. From SEM micrographs, surface nucleation along grain boundaries appears to be the dominant mode.

2. FTi.r. absorption spectra have been shown to be capable of providing both qualitative and quantitative characterization of crystal nucleation and growth in the annealed frit-S and the non-borate base glass-S. The FTi.r. method consists of: (a) the selection of a specific i.r. absorption peak position at 564 cm^{-1} for SiO_4, (b) calibration by the classical least square method, using high-purity/crystallinity materials as standards, amount (wt %) versus peak height, obtaining correlation coefficients of > 0.993; and (c) derived amount (wt %) from calibration plot. Similar quantitative FTi.r. studies for a broader scope of glass compositions are to be encouraged so that the application of FTi.r. spectroscopy in glass–ceramics may be advanced.

3. Activation energies, E_c, of crystal nucleation/growth may be estimated by two different methods, namely via DTA data and FTi.r. absorption spectra. E_c for $CaTiSiO_5$, β-$CaSiO_3$ and α-cristobalite in the frit-S and a non-borate base glass-S are estimated to be 219.6, 107.2 and 51.5 kJ mol^{-1}, respectively, parallel to the decreasing order of chemical complexity of the glass-forming system: (a) sphene, $CaTiSiO_5$, (b) β-wollastonite, $CaSiO_3$; and (c) α-cristobalite, SiO_2. Also, similar values of E_c for sphene in two chemically similar test materials are separately obtained as: (a) 219.6 kJ mol^{-1} in frit-S, directly based on FTIR absorption spectra, and (b) 224.0 kJ mol^{-1} in the non-borate based glass-S, indirectly derived.

Acknowledgements

We wish to express our appreciation to the National Science Council, Taiwan, R.O.C., for providing financial support for this investigation (NSC 82–0405–E–006–204). We also wish to deeply thank Professors F. S. Yen, M. H. Hon, M. C. Wang and C. Y. Huang for their interest and guidance.

References

1. D. M. SANDERS, W. B. PERSON and L. L. HENCH, *Appl. Spectrosc.* **28** (1974) 247.
2. A. PUTNIS and D. L. BISH, *Amer. Mineral.* **68** (1983) 60.
3. D. M. HAALAND, in "Practical Fourier Transform Infrared Spectroscopy-Industrial and Laboratory Chemical Analysis" edited by J. R. Ferraro and K. Krishnan (Academic Press, California, 1990) pp. 395–469.
4. S. K. CHEN, H. S. LIU and C. S. WU, *Appl. Spectrosc.* **47** (1993) 965
5. J. R. TAYLOR and A. C. BULL, "Ceramic Glaze Technology" (Pergamon press, Oxford, 1986) pp. 50–62.

6. W. A. DEER, R. A. HOWIE and J. ZUSSMAN, "Rock-Forming Minerals" Vol. 1A (Longman, Harlow, 1977) pp. 443–466.
7. E. R. VANCE, P. J. HAYWARD, J. C. TAIT, I. M. GEORGE and A. A. CARMICHAEL, *Amer. Ceram. Soc. Bull.* **65** (1986) 1423.
8. F. C. HAWTHORNE et al., *Amer. Mineral.* **76** (1991) 370.
9. J. S. HARTMAN, R. L. MILLARD, E. R. VANCE, *J. Mater. Sci.* **25** (1990) 2785.
10. Q. WILLIAMS and T. F. COONEY, *Amer. Mineral.* **77** (1992) 1.
11. A. M. HOFMEISTER and A. CHOPELAS, *Phys. Chem. Minerals*, **17** (1991) 503.
12. M. H. MANGHNANI, J. R. FERRARO and L. J. BASILE, *Appl. Spectrosc.* **28** (1974) 256.
13. C. HUANG and E. C. BEHRMAN, *J. Non-Cryst. Solids* **128** (1991) 310.
14. M. GABELICA-ROBERT and P. TARTE, *Phys. Chem. Minerals* **7** (1981) 26.
15. S. A. BRAWER and W. B. WHITE, *J. Non-Cryst. Solids* **23** (1977) 261.
16. B. O. MYSEN, D. VIRGO and F. A. SEIFERT, *Amer. Mineral.* **70** (1985) 88.
17. F. GERVAIS, A. BLIN, D. MASSIOT, J. P. COUTURES, M. H. CHOPINET and F. NAUDIN, *J. Non-cryst. Solids* **89** (1987) 384.
18. P. McMILLAN and B. PIRIOU, *ibid.* **53** (1982) 279.
19. M. HASS, *J. Phys. Chem. Solids* **31** (1970) 415.
20. R. C. DeVRIES, R. ROY and E. F. OSBORN, *J. Amer. Ceram. Soc.* **38** (1955) 161.
21. P. J. HAYWARD, E. R. VANCE and D. C. DOERN, *Amer. Ceram. Soc. Bull.* **66** (1987) 1620.
22. M. J. BUERGER, in "Transactions of the American Crystallographic Association" Vol. 7, edited by S. Block (Polycrystal Book Service, Pittsburgh, 1971) pp. 1–23.
23. J. ZARZYCKI, in "Advances in Ceramics" Vol. 4, edited by J. H. Simmons, D. R. Uhlmann and G. H. Beall (American Ceramics Society, Ohio, 1982) pp. 204–214.
24. A. MAROTTA, A. BURI and G. L. VALENT, *J. Mater. Sci.* **13** (1978) 2483.
25. A. MAROTTA, A. BURI, F. BRANDA and S. SAIELLO, in "Advances in Ceramics" Vol. 4, edited by J. H. Simmons, D. R. Uhlmann and G. H. Beall (American Ceramics Society, Ohio, 1982) pp. 146–152.
26. P. F. JAMES, in "Advances in Ceramics" Vol. 4, edited by J. H. Simmons, D. R. Uhlmann and G. H. Beall (American Ceramics Society, Ohio, 1982) pp. 1–48.
27. M. C. WANG and M. H. HON, *J. Ceram. Soc. Jpn.* **100** (1992) 1285.

Received 11 May
and accepted 30 November 1993